

Supporting information for

Fabrication Novel Nanofiltration Membrane using Mg-Fe Layered Double Hydroxide for dye/salt separation

Xiuzhen Wei^{1*}; Zelong Chen¹; Mengjia He¹; Liangliang Xu¹; Yue Li¹; Jia Yang²;
Xuekang Zhang¹; Xianghao Zhang¹; Ze Wang¹, Shiyu Cao¹, Qinghua Zhou^{1,*};
Bingjun Pan^{1*}

¹College of Environment, Zhejiang University of Technology, Hangzhou,
310014, China

²Ninghai Society of Environmental Science and Technology, Ningbo, Zhejiang,
315600, China

* Corresponding author, Xiuzhen Wei College of Environment, Zhejiang University of Technology, E-mail: xzwei@zjut.edu.cn

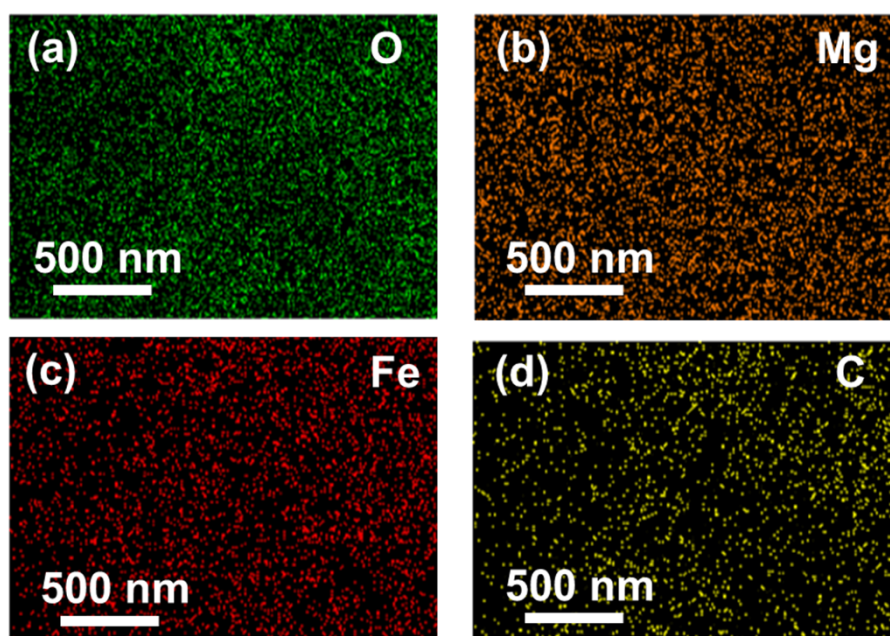
* Corresponding author, Qinghua Zhou College of Environment, Zhejiang University of Technology, E-mail: qhzhou@zjut.edu.cn

* Corresponding author, Bingjun Pan College of Environment, Zhejiang University of Technology, E-mail: bjpan@zjut.edu.cn.

1. NF membrane preparation condition optimization

1 The influence of membrane preparation conditions on the membrane performance
2 was studied. In order to obtain NF membrane with optimal separation performance,
3 the concentration of PIP, TMC, Mg-Fe LDH, heat treatment time, and heat treatment
4 temperature were optimized based on the permeation flux and rejection rate for 1000
5 $\text{mg}\cdot\text{L}^{-1}$ Na_2SO_4 solution.

6 1.1 Element mapping images of Mg-Fe LDH



7
8 **Fig. S1** (a) O, (b) Mg, (c) Fe, and (d) C element mapping images of Mg-Fe LDH
9

10 1.2 FT-IR spectra of Mg-Fe LDH

11

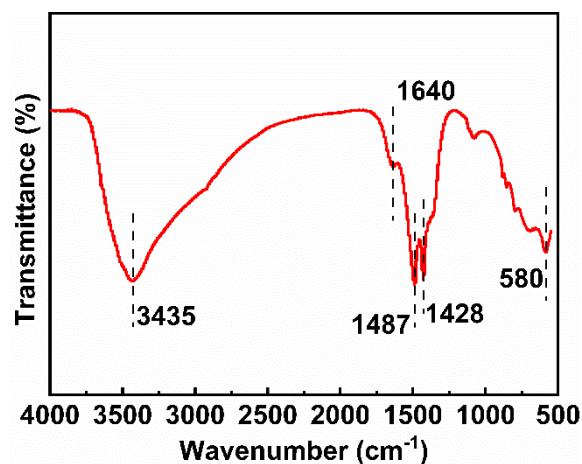


Fig. S2 FT-IR spectra of Mg-Fe LDH

12
13
14

15 1.3 Wide-scan XPS analysis spectra of different NF membranes

16

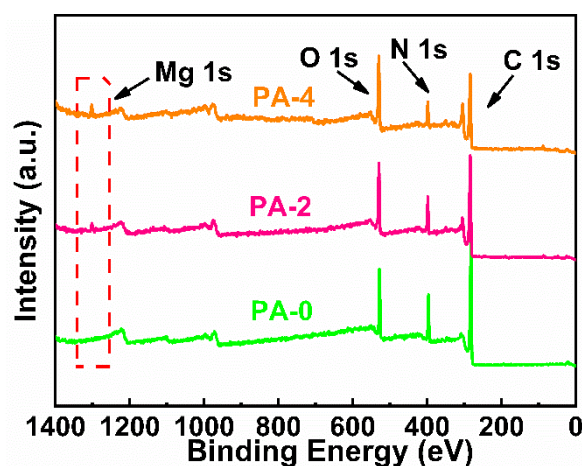


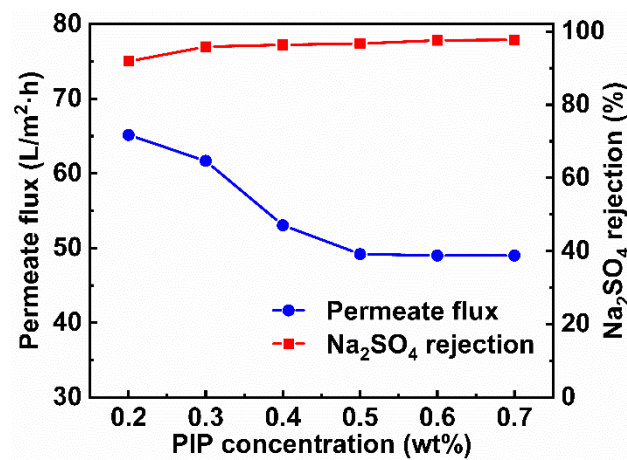
Fig. S3 Wide-scan XPS analysis spectra of different NF membranes

17
18
19

20 1.4 The effect of PIP concentration

21 PIP concentration will directly affect the thickness of the selective layer. The effect
 22 of aqueous PIP concentration on NF separation performance was investigated firstly
 23 and the results were shown in Fig. S4. TMC concentration was fixed at 0.15 wt%,
 24 Mg-Fe LDH concentration was 0.1 wt%, heat treatment temperature was 60 °C and
 25 heat treatment time was 10 min when PIP concentration was changed. As shown in
 26 Fig. S4, the permeation flux of Mg-Fe LDH modified NF membrane for Na₂SO₄

27 gradually decreases with the increase of the PIP concentration, while the rejection rate
28 for Na_2SO_4 increased continuously. With the increase of PIP concentration, the
29 number of PIP molecules fixed into the selective layer increased due to TMC
30 concentration being fixed, the effective thickness of the selective layer increases
31 correspondingly which led to the decrease of permeation flux and the increase of
32 rejection rate. Considering the permeation flux and rejection rate of the NF membrane,
33 the optimal concentration of PIP in this study was chosen as 0.3 wt%.
34

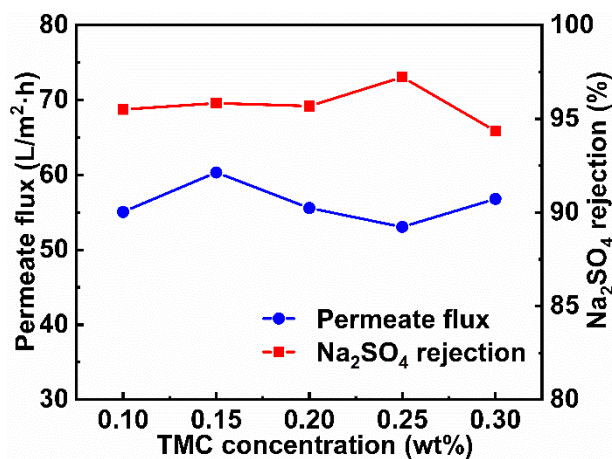


35
36 **Fig. S4** Effect of PIP concentration on Mg-Fe LDH modified NF membrane
37 performance.

38 1.5 The effect of TMC concentration

39 TMC concentration will directly determine the compactness of the selective layer.
40 When Mg-Fe LDH concentration was fixed at 0.1 wt%, PIP concentration was 0.3
41 wt%, heat treatment temperature was 60 °C and heat treatment time was 10 min, the
42 effect of TMC concentration on NF separation performance was investigated and the
43 results were shown in Fig. S5. As shown in Fig. S5, when the TMC concentration was
44 lower than 0.15 wt%, the permeation flux of Mg-Fe LDH modified NF membrane to
45 the Na_2SO_4 solution increased with TMC concentration increase and the salt rejection
46 rate kept relatively stable. However, when the TMC concentration range in 0.15-0.25
47 wt%, the permeation flux decreases gradually accompanied by the rejection rate
48 increase slightly. When TMC concentration was higher than 0.25 wt%, the

49 permeation flux increases obviously, and the rejection rate decreases sharply. If the
50 concentration of TMC was lower than 0.15 wt%, the reaction was not complete and
51 the crosslinking rate of the functional layer was not good. Along with the addition of
52 TMC concentration, the crosslinking rate of the functional layer gets better, the
53 surface of the composite layer becomes rougher. As a result, the contacting area of the
54 membrane and water was larger, which promotes the mass transfer of water^[1]. As
55 TMC concentration increases (higher than 0.15 wt%), the cross-linking degree of the
56 functional layer increases which leads to increases in rejection rate and the decrease
57 of permeation flux. However, if TMC concentration was too high (higher than 0.25
58 wt%), the interfacial polymerization reaction became too fast, the formed cross-
59 linking functional layer will relatively loose and the cross-linking structure presents
60 some defects. Some unreacted acyl chloride groups will hydrolyze to carboxyl groups,
61 which causes the permeate flux of the membrane to increase and improves the
62 hydrophilicity of the membrane^[2].
63



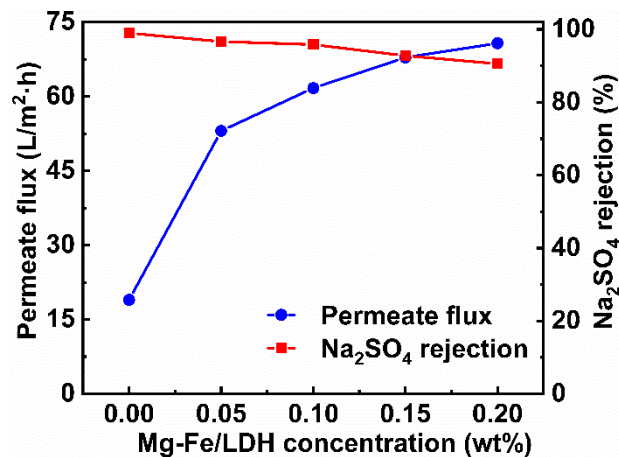
64
65 **Fig. S5** Effect of TMC concentration on Mg-Fe LDH modified NF membrane
66 performance

67 1.6 The effect of Mg-Fe LDH concentration

68 The presenting of nanoparticles LDH will affect the morphology and structure of
69 NF membranes. The effect of Mg-Fe LDH concentration on NF separation
70 performance was investigated when PIP concentration was 0.3 wt%, TMC

71 concentration was 0.15 wt%, heat treatment temperature was 60 °C, heat treatment
72 time was 10 min. As it can be seen from Fig.S6, the permeation flux of modified NF
73 membrane increases with Mg-Fe LDH concentration increase very obviously, and the
74 rejection rate for Na₂SO₄ decreases slightly. The flux improvement was contributed to
75 the addition of Mg-Fe LDH to provide additional channels for water molecule
76 transportation. At the same time, the hydrophilicity of the NF membrane was
77 improved obviously due to Mg-Fe LDH molecules having abundant hydroxyl groups,
78 which can promote and increase the absorption of water molecules on the NF
79 membrane surface^[3]. However, accompanied by an LDH loading increase, the
80 rejection rate of the membrane decreased slightly, which may be due to LDH
81 providing an additional transport channel and forming some defects in the selective
82 layer. Considering the permeation flux and rejection rate of the NF membrane, the
83 optimized Mg-Fe LDH concentration was chosen as 0.1 wt%.

84



85

86

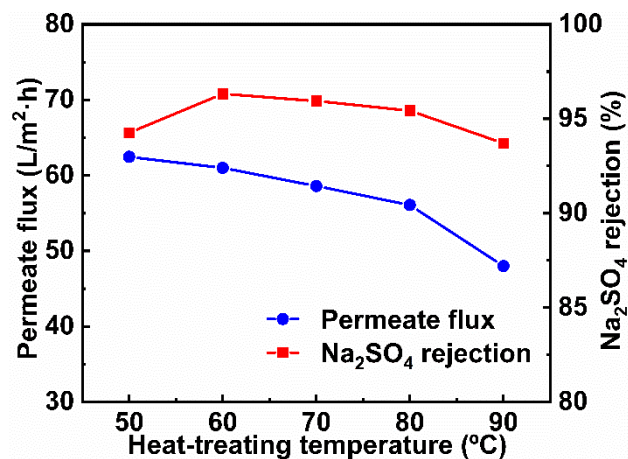
Fig. S6 Effect of Mg-Fe LDH concentration on NF membrane performance

87 1.7 Effect of heat treatment temperature

88 When Mg-Fe LDH concentration was fixed at 0.1 wt%, PIP concentration was 0.3
89 wt%, TMC concentration was 0.15 wt%, and the heat treatment time was 10 min, the
90 effect of heat treatment temperature on NF membrane separation performance was
91 investigated and the results are shown in Fig. S7. With the increase of the heat

92 treatment temperature, the permeation flux of the NF membrane decreases gradually,
93 and the rejection rate increase firstly and then decreases slowly. To some degree, the
94 increase of temperature can improve interfacial polymerization reaction, which leads
95 to the cross-linking degree of selective functional layer increase and makes the
96 selective layer denser. However, if the temperature was too high, some chemical
97 bonds and hydrogen bonds of the cross-linking selective layer will break, and some
98 defects will be formed, which lead to the reduction of the rejection rate. Considering
99 the permeate flux and rejection rate of the NF membrane, the heat treatment
100 temperature was fixed at 60°C in the following study.

101



102

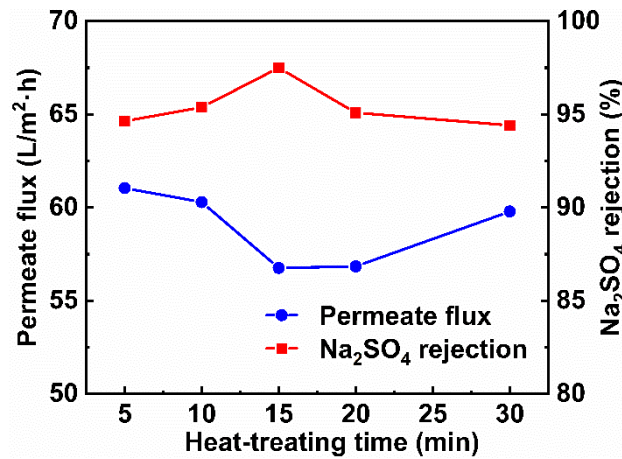
103 **Fig. S7** Effect of heat treatment temperature on NF membrane performance

104 **1.8 Effect of heat treatment time**

105 Effect of heat treatment time on NF membrane separation performance was
106 investigated when Mg-Fe LDH concentration was fixed at 0.1 wt%, PIP concentration
107 was 0.3 wt%, TMC concentration was 0.15 wt%, and the heat treatment temperature
108 was 60°C. As it can be seen from Fig.S8, with the increase of heat treatment time the
109 rejection rate of Na₂SO₄ increased firstly and then decreased. However, accompanied
110 by the change of rejection rate, the permeation flux presented an opposite change
111 trend. The heat treatment process will accelerate the interface polymerization reaction
112 speed. If the heat treatment time was less than 15 min, with heat treatment time

113 prolonging, PIP and TMC will be crosslinked further, which lead the formed selective
114 functional layer denser. As a result, the membrane permeation flux decreased and the
115 salt rejection rate increased. However, as the heat treatment time continues to increase,
116 some cracks and defects will appear in the selective functional layer due to the
117 expansion coefficients of the selective layer and the support layer being different,
118 which contributed to the increase of permeation flux and the decrease the rejection
119 rate. Considering the permeate flux and rejection rate of the NF membrane, the heat
120 treatment time was fixed at 10 min.

121



122

123 **Fig. S8** Effect of heat treatment time on Mg-Fe LDH modified NF membrane.

124

125

126

127

128

129

130

131

132

133

134

135
136
137
138
139
140

Table S1 Preparation conditions of different NF membrane

Membrane	LDH (wt%)	PIP (wt%)	TMC (wt%)	Heat treatment temperature (°C)	Heat treatment time (min)
PA-0	0	0.3	0.15	60	10
PA-1	0.05	0.3	0.15	60	10
PA-2	0.1	0.3	0.15	60	10
PA-3	0.15	0.3	0.15	60	10
PA-4	0.2	0.3	0.15	60	10

141
142
143
144
145

Table S2 The molecular weight and molecular radius of PEG

Solute	Molecular Weight	r_s
PEG-200	200.00	0.64
PEG-400	400.00	0.94
PEG-600	600.00	1.18
PEG-800	800.00	1.38
PEG-1000	1000.00	1.56

146
147
148
149
150
151
152
153

154
155
156
157
158

Table S3 Surface chemical compositions of different NF membranes

Membrane	Surface chemical compositions (At.%)				
	C	O	N	Mg	Fe
PA-0	73.70	13.27	13.04	-	-
PA-2	70.37	16.17	11.57	1.42	0.47
PA-4	60.09	22.48	11.63	4.34	1.46

159
160
161
162

Table S4 Roughness of different NF membranes

Membranes	Ra (nm)	RMS (nm)
PA-0	4.99	6.58
PA-2	2.94	3.71
PA-4	2.43	2.98

163
164
165
166

Table S5 Characteristic parameters of different membranes

Membrane	PWP ($L \cdot m^{-2} \cdot h^{-1}$)	MWCO (Da)	μ_p (nm)	ρ_p
PSF	800	50,000	3	-
PA-0	30.1 ± 0.3	281	0.415	1.53
PA-2	70.4 ± 1.1	385	0.493	1.69
PA-4	80.8 ± 0.4	597	0.559	1.75

167

168

169

170

Table S6 Property comparison of different nanomaterial-modified NF membrane

	Nanomaterials	Reactive monomer	Flux ($L \cdot m^{-2} \cdot h^{-1} \cdot bar^{-1}$)	Rejection rate (%)	Contaminant	Reference
1	ODA-h-NCs	PIP/TMC	8.97	95.8	Na ₂ SO ₄	[4]
2	AgNPs	MPD/TMC	10.4	97.7	Na ₂ SO ₄	[5]
3	MWCNTs-OH	PIP/TMC	6.9	97.6	Na ₂ SO ₄	[6]
4	O-MoS ₂	PIP/TMC	7.91	97.9	Na ₂ SO ₄	[7]
5	rGO/TiO ₂	PIP/TMC	6.0	93.6	Na ₂ SO ₄	[8]
6	r-GO	PIP/TMC	6.6	98.5	Na ₂ SO ₄	[9]
7	GO	PIP/TMC	10.4	94.6	Na ₂ SO ₄	[10]
8	GO/MWCNTs	PIP/TMC	13.9	94.0	Na ₂ SO ₄	[10]
9	Blank	PIP/TMC	5.7	98.9	Na ₂ SO ₄	This work
10	Mg-Fe LDH	PIP/TMC	15.2	96.4	Na ₂ SO ₄	This work

171

172

References

- 173 [1] Lau W J, Ismail A F, Misdan N et al (2012) A recent progress in thin film
174 composite membrane: A review. *Desalination* 190-199.
- 175 [2] Wang Q, Zhang G S, Li Z S et al (2014) Preparation and properties of
176 polyamide/titania composite nanofiltration membrane by interfacial polymerization.
177 *Desalination* 38-44.
- 178 [3] Tian X, Wang J, Zhang H et al (2018) Establishment of transport channels with
179 carriers for water in reverse osmosis membrane by incorporating hydrotalcite into the
180 polyamide layer. *RSC Advances* 12439-12448.
- 181 [4] Istirokhatun T, Lin Y Q, Shen Q, Guan K C, Wang S Y, Matsuyama H. Ag-
182 based nanocapsule-regulated interfacial polymerization Enables synchronous
183 nanostructure towards high-performance nanofiltration membrane for sustainable
184 water remediation. *Journal of Membrane Science*, 2022, 645:120196-120205.
- 185 [5] Xue S M, Xu Z L, Tang Y J, Ji C H. Polypiperazine-amide nanofiltration
186 membrane modified by different functionalized multiwalled carbon nanotubes
187 (MWCNTs), *ACS Applied Materials & Interfaces*, 2016, 8(29): 19135-19144.
- 188 [6] Yang S S, Jiang Q L, Zhang K S. Few-layers 2D O-MoS₂ TFN nanofiltration
189 membranes for future desalination. *Journal of Membrane Science*, 2020, 604:118052-
190 118063.
- 191 [7] Chen X Y, Feng Z H, Gohil J, Stafford C M, Dai N, Huang L, Lin H Q.
192 Reduced holey graphene oxide membranes for desalination with improved water
193 permeance. *Acs Applied Materials & Interfaces*, 2020, 12, (1), 1387-1394.
- 194 [8] Safarpour M, Vatanpour V, Khataee A, Esmaeili M. Development of a novel
195 high flux and fouling-resistant thin film composite nanofiltration membrane by
196 embedding reduced graphene oxide/TiO₂, *Separation and Purification Technology*,
197 2015, 154: 96-107.
- 198 [9] Chen X Y, Feng Z H, Gohil J, Stafford C M, Dai N, Huang L, Lin H Q.
199 Reduced holey graphene oxide membranes for desalination with improved water
200 permeance. *Acs Applied Materials & Interfaces*, 2020, 12, (1), 1387-1394.
- 201 [10] Tian X, Wang J, Zhang H, Cao Z, Zhao M, Guan Y, Zhang Y. Establishment
202 of transport channels with carriers for water in reverse osmosis membrane by
203 incorporating hydrotalcite into the polyamide layer, *RSC Advances*, 2018, 8(22):
204 12439-12448.